Active Magnetic and Touchdown Bearings to Encourage Rotor Re-Levitation from a Persistent Contact Condition

Peichao Li
University of Bath
Bath, UK

M. Necip Sahinkaya
University of Bath
Bath, UK

Patrick S. Keogh*
University of Bath
Bath, UK

Abstract

Magnetic bearing systems are commonly used for high speed rotor applications, having particular advantages in low pressure/vacuum environments. The benefits of using magnetic bearing systems are well documented in terms of low fiction and controllable stiffness and damping. In order to protect magnetic bearings in cases of power failure, intermittent faults and unexpected external disturbances, secondary back-up or touchdown bearings are usually included so that rotor/stator contact is prevented. If, for any reason, a rotor should make contact with a touchdown bearing, the ensuing rotor dynamic response will depend on operational parameters and any residual rotor unbalance distribution. The influence of unbalance force distributions on the contact rotor dynamics are demonstrated in this paper. Interactions between a rotor and touchdown bearings can cause relatively high contact forces that could be damaging in terms of direct mechanical stresses and through induced heat inputs when slip occurs. In order to alleviate the contact problem an actively controlled touchdown bearing system has been proposed to reduce contact forces and, where possible, recover rotor positional control and return it to a condition of contact-free levitation. Active touchdown bearing control may be applied together with magnetic bearing control and suggested strategies to encourage rotor contact-free levitation are assessed in this paper.

1 Introduction

The existence of unbalance force distributions together with changing operating conditions and external disturbances will require consideration of a magnetically levitated rotor making contact with one or more touchdown bearings. The issues associated with rotor/touchdown bearing contact have been studied by many researchers [1]. For the same rotor assembly, contact and non-contact rotor dynamics may co-exist. Within a bearing clearance, non-linear dynamics associated with contact are reported in [2-4], while the rotor dynamics involving rub and bounce-like motions have been presented in [5-9]. The main purpose of touchdown bearings is to keep a rotor strictly within the clearance circles of magnetic bearings, thereby protecting rotor and stator interfaces. A touchdown bearing is regarded as a sacrificial component. In the event of power loss, the rotor will drop onto the touchdown bearing without levitation control. Rotor drop tests to investigate this have been carried out by a number of researchers [10-14]. High dynamic contact forces have been observed in [15-18]. The transient behavior of a rotor during contact has been identified by researchers in [19-21]. Other researches have investigated procedures to reduce contact forces, either using magnetic bearing control [22, 23], or touchdown bearing motion [24, 25] through electromagnetic actuation. Consideration of procedures to regain contact-free control of a functioning rotor/magnetic bearing system through piezoelectric actuation of an active touchdown bearing is reported in [26, 27].

A well-controlled rotor should never make contact with a touchdown bearing if the unbalance distribution is sufficiently low and rotor vibration amplitudes remain within clearance limits at all times. However, at certain speeds and unbalance conditions, the rotor may co-exist in stable orbits; one without contact and others involving persistent touchdown bearing interactions. An external disturbance could cause the transition from the contact-free orbit to a persistent contact case. In principle, another external disturbance could reverse the transition back to the contact-free orbit. This paper focuses on a control method that uses both the active magnetic and touchdown bearings to encourage a rotor back to a contact-free orbit condition. For a flexible rotor with an uncertain unbalance distribution, the rotor may make contact with more than one touchdown bearing. This paper will demonstrate the feasibility of using magnetic bearing control and active touchdown bearing control to bring the rotor contact-free operation, effectively by applying appropriate disturbances to the rotor.

*Contact Author Information: enspsk@bath.ac.uk, Tel: +44 (0)1225 385958, Fax: +44 (0)1225 386928

2 Nomenclature

$\mathbf{B}$ = transformation matrix
c_m, c_t = magnetic bearing, touchdown bearing clearance
$\mathbf{C}$ = damping matrix
$\mathbf{e}_u$ = unbalance eccentricity vector
f_m = magnetic bearing force from opposing coil pairs
f_t = touchdown bearing contact force
$\mathbf{f}$ = force vector
$\mathbf{f}_{t,t}$ = tangential contact force
$\mathbf{f}_{t,n}$ = normal contact force
$\mathbf{G}$ = gyroscopic matrix
k_m = magnetic bearing force coefficient
k_{me}, c_{me} = magnetic bearing equivalent stiffness, damping
k_{te}, c_{te} = touchdown bearing equivalent stiffness, damping
$\mathbf{K}$ = stiffness matrix
l_t = axial length of touchdown bearing
m = mass
$\mathbf{m}_u$ = unbalance mass matrix
$\mathbf{M}$ = mass matrix
q_m = magnetic bearing radial clearance gap
q_r = rotor radial displacement
q_t = touchdown bearing radial clearance gap
$\mathbf{q}$ = rotor displacement vector
r = radius
r_{do}, r_{di} = rotor outer, inner radii

Ω = rotational speed
θ = rotational angle displacement
i_0 = bias current
i = magnetic bearing coil current
μ = friction coefficient
δ_r = rotor displacement relative to touchdown bearing
ν = Poisson ratio
E = Young's modulus

Subscripts
r = rotor
u = unbalance
m = magnetic bearing
t = touchdown bearing
d = disk
ux, uy = unbalance in *x*, *y* direction
at = actively controlled touchdown bearing

3 System Description

The rotor dynamics will be for an established test rig (Figure 1(a)). It consists of:

(a) Two active magnetic bearings (AMBs), each formed by four coil pairs arranged orthogonally to each other. As shown in Figure 1(b), control axes are arranged at ±45 degrees to the vertical to achieve the highest static vertical force capacity. Each AMB control axis has a force capacity of 500 N and a break frequency of 250 Hz.
(b) Two touchdown bearings (TDBs) adjacent to and outboard of the magnetic bearings. Each TDB is a ball bearing type, which may pushed by four hydraulic pistons in control axes similar to those of the magnetic

bearings, as shown in Figure 1(c). The actuation force from each piston is provided by a piezoelectric stack actuator through a closed hydraulic line. Each piezoelectric actuator has a blocking force of 12,000 N and a bandwidth of 4,000 Hz. The active TDB bandwidth is reduced to 800 Hz due to the compressibility effect of the hydraulic fluid.

(c) A rotor consisting of a shaft of length 800 mm, diameter 30 mm and made from stainless steel, on which are mounted three disks with balance holes at a radius of 35 mm. Rotor laminations are also mounted on the shaft.

(d) An electric motor to drive the shaft though a flexible bellows coupling, up to 10,000 rpm.

The layout of the test rig is shown in Figure 1(d). The AMBs are located inboard of the TDBs for better protection on the AMBs if the rotor is in its first flexural mode. Each AMB has a radial clearance of 0.8 mm, while each TDB has a radial clearance of 0.4 mm.

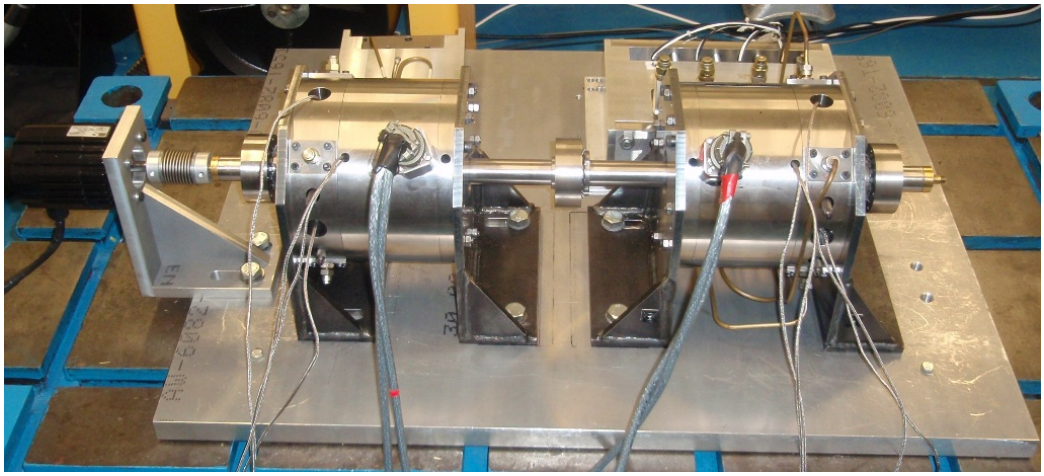

(a) Test Rig

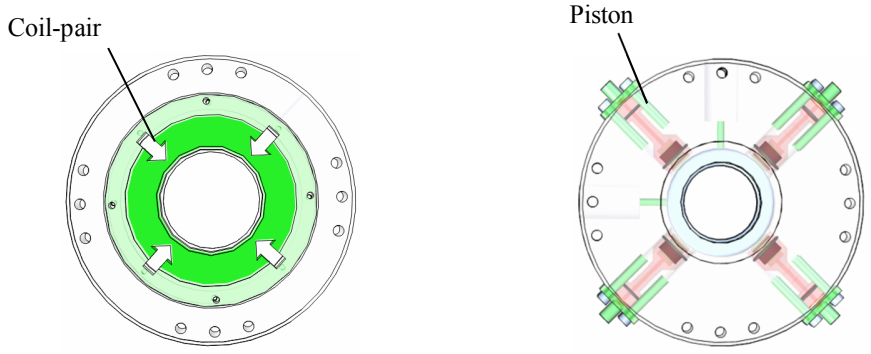

(b) AMB (c) TDB

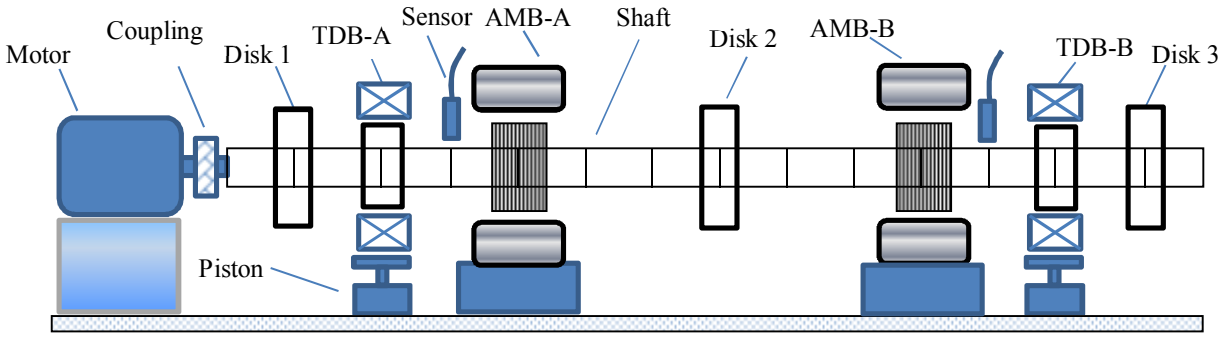

(d) Test rig arrangement

Figure 1. Active magnetic bearing (AMB) and touchdown bearing (TDB) system

4 Model of the System

The dynamics of the rotor assembly are expressed in finite element form according to [28]:

$$\mathbf{M}_r\ddot{\mathbf{q}}_r + \Omega\mathbf{G}_r\dot{\mathbf{q}}_r + \mathbf{K}_r\mathbf{q}_r = \mathbf{B}_u\mathbf{f}_u + \mathbf{B}_m\mathbf{f}_m + \boldsymbol{B}_t\boldsymbol{f}_t \tag{1}$$

where $\mathbf{q}_r$ is the vector of node translational and angular displacements, $\mathbf{M}_r$, $\mathbf{G}_r$ and $\mathbf{K}_r$ are the mass, gyroscopic and stiffness matrices of the rotor, respectively, Ω is the rotor rotational speed, $\mathbf{f}_u$, $\mathbf{f}_m$ and $\mathbf{f}_t$ are the unbalance force, magnetic bearing force and touchdown bearing contact force vectors, respectively. $\mathbf{B}_u$, $\mathbf{B}_m$ and $\mathbf{B}_t$ are transformation matrices to distribute the local force vectors to the global coordinates in $\mathbf{q}_r$.

The unbalance force vector is

$$\mathbf{f}_u = [\mathbf{f}_{ux}^{\boldsymbol{T}}, \quad \mathbf{f}_{uy}^{\boldsymbol{T}}]^{\boldsymbol{T}} \tag{2}$$

where, for zero phasing,

$$\mathbf{f}_{ux} = \mathbf{m}_u\mathbf{e}_u(\Omega^2\cos\theta + \dot{\Omega}\sin\theta)\,, \mathbf{f}_{uy} = \mathbf{m}_u\mathbf{e}_u(\Omega^2\sin\theta - \dot{\Omega}\cos\theta) \tag{3}$$

and

$$\theta = \int_0^t \Omega(\tau)d\tau \tag{4}$$

Here, $\mathbf{m}_u$ is the unbalance mass vector, $\mathbf{e}_u$ is the unbalance mass radial offset vector. The rotor is not considered to undergo any rapid speed changes, hence $\dot{\Omega}$ will be very small compared to the Ω^2 term. The unbalance force equation therefore reduces to the usual form of

$$\mathbf{f}_{ux} = \mathbf{m}_u\mathbf{e}_u\Omega^2\cos\theta \tag{5}$$

$$\mathbf{f}_{uy} = \mathbf{m}_u\mathbf{e}_u\Omega^2\sin\theta \tag{6}$$

The non-linear AMB force in a control axis is expressed in the usual form involving opposing coil pairs:

$$f_m = k_m\left(\frac{(i_0+i)^2}{(q_m-q_r)^2} - \frac{(i_0-i)^2}{(q_m+q_r)^2}\right) \tag{7}$$

where k_m is the magnetic bearing force coefficient, which depends on the physical parameters of the magnetic bearing. Also, i_0 and i are the bias and electrical control currents, respectively, q_m is the radial clearance or nominal air gap, and q_r is the rotor radial displacement from the center of the bearing.

The contact force vector $\mathbf{f}_t$ includes the normal contact force $\mathbf{f}_{t,n}$ and the tangential force vector $\mathbf{f}_{t,t}$, which are related by

$$\mathbf{f}_{t,t} = \mu\mathbf{f}_{t,n} \tag{8}$$

where μ is the friction coefficient between the rotor and the TDB. The contact force calculation is made using a backward evaluation from a Hertzian contact model. Contact only occurs if the rotor relative radial displacement δ_r to the touchdown bearing exceeds the clearance gap of the touchdown bearing q_t:

$$\delta_r - q_t \geq 0 \tag{9}$$

The amplitude of contact force f_t at a single position is given by

$$\delta_r - q_t = \frac{2f_t(1-\nu)}{\pi E l_t}\left(\frac{2}{3} + ln\frac{8Eq_tl_t}{2.15^2f_t}\right) \tag{10}$$

where ν is the Poisson ratio, E is Young's modulus and l_t is the axial length of contact zone between the rotor and TDB. The contact force is calculated from Equation (10) using an inverse numerical method.

The TDBs are of ball bearing type, supported by four hydraulic pistons. The support material and ball bearings are considered to have stiffness and damping characteristics. The equation of motion of the system of TDBs is expressed as

$$\mathbf{M}_t\ddot{\mathbf{q}}_t + \mathbf{C}_t\dot{\mathbf{q}}_t + \mathbf{K}_t\mathbf{q}_t = \mathbf{f}_{at} - \mathbf{f}_t \tag{11}$$

where $\mathbf{q}_t$ is the TDB radial displacement vector, $\mathbf{M}_t$, $\mathbf{C}_t$ and $\mathbf{K}_t$ are the mass, damping and stiffness matrices, and $\mathbf{f}_{at}$ is the effective controlled force vector arising from the piezoelectric actuators. If $\mathbf{f}_{at} = 0$, the TDBs operate in a passive mode. The contact force $\mathbf{f}_t$ is considered with the negative sign in Equation (11) to reflect the fact that it acts in the opposite direction to rotor radial displacement.

5 Simulation and Results

The data in Table 1 were used in the simulation of the system. Firstly, the unbalance mass m_u was considered to be added to Disk 1. Then the rotor rotational speed was slowly increased from 0 to 3,000 rad/s. The rotor radial displacements at TDB-A and TDB-B (Figure 1) were evaluated to identify the critical operating speed of the rotor assembly. In the calculation, the linearized AMB equivalent stiffness and damping coefficients were applied directly to the rotor. The same calculation was then repeated with two unbalance masses attached to Disk 1 and Disk 2, then again for unbalance masses on Disks 1, 2 and 3. Figures 2(a) and 2(b) show the slow run-up rotor radial displacement at TDBs A and B, respectively, assuming that no contact occurs. Several critical speeds are noted, the most obvious one is at around 840 rad/s, which corresponds to the first flexural mode of the rotor. The rigid body critical speed below the first flexural mode is well damped by the magnetic bearings. The critical speed at around 2,200 rad/s corresponds with the second flexural mode, which is well above the motor operating speed of 10,000 rpm. Figure 2 also shows that the critical speed at 2,200 rad/s is not obvious when three disks are unbalanced. The rotor radial displacement is its highest around the first flexible critical speed at both TDB positions. The rotor radial displacement would exceed the TDB clearance of 0.4 mm, hence the rotor assembly with three unbalanced disks at around operating speed of 840 rad/s will be the focus of further simulations. It could be argued that the maximum radial displacement is larger than the half of the magnetic bearing clearance hence it is not realistic to use equivalent linearized magnetic bearing stiffness and damping. Time domain simulation was therefore undertaken using the non-linear magnetic bearing model of Equation (7) over speeds between 740 rad/s and 940 rad/s. The results matched well with those of Figure 2.

Parameter	Symbol	Value
Rotor assembly mass	m	10 kg
Rotor radius	r_r	15 mm
Rotor disk mass	m_d	1.08 kg
Rotor disk outer radius	r_{do}	40 mm
Rotor disk inner radius	r_{di}	15 mm
Unbalance mass	m_u	variable
Unbalance offset distance	e_u	35 mm
Magnetic bearing clearance	c_m	0.8 mm
Magnetic bearing force coefficient	k_m	5.8 $\mu Nm^2/A^2$
Magnetic bearing equivalent stiffness	k_{me}	$6x10^5$ N/m
Magnetic bearing equivalent damping	c_{me}	1760 Ns/m
TDB clearance	c_t	0.4 mm
TDB width	l_t	30 mm
TDB radius	r_t	25 mm
TDB equivalent stiffness	k_{te}	$6x10^7$ N/m
TDB equivalent damping	c_{te}	2450 Ns/m
Rotor/TDB coefficient of friction	μ	0.15

Table 1: System Parameters

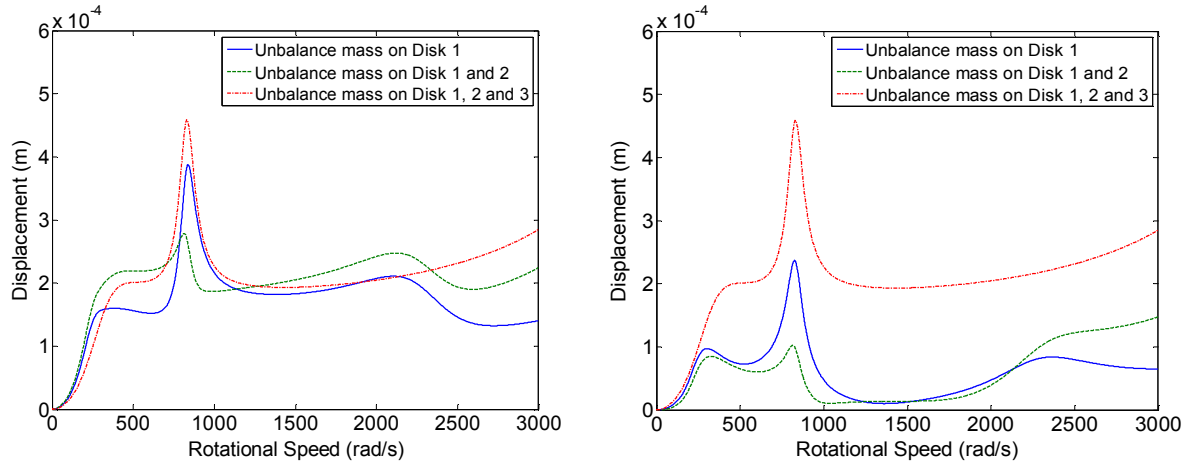

(a) Rotor radial displacement at TDB-A (b) Rotor radial displacement at TDB-B

Figure 2: Steady Rotor Response at TDB locations due to Unbalance Distributions with m_u = 13.5 g

It is predicted from Figure 2 that the rotor will make contact with a TDB with three unbalance masses of 13.5 g and offset by 35 mm between speeds of 740 rad/s and 940 rad/s. Time domain simulation was therefore undertaken with the TDBs included for contact force contributions. The results include rotor radial displacement and operating speed as shown in Figure 3. It shows the rotor starts to make contact with the TDBs as the speed increases. After initial bouncing contact the rotor makes continuous contact with TDB-A and enters a full rub condition. The contact continues up to 940 rad/s, beyond which the results of Figure 2 indicate no contact. Hence there could be two stable and co-existing orbits for the rotor at 940 rad/s. Due to some external disturbance, the rotor could enter the full rub contact mode from contact-free levitation or vice-versa.

It would be beneficial to use AMB and/or TDB control to keep the rotor in contact-free levitation. The AMB control will now consider the standard balancing approach developed in [29, 30] to generate control forces to reduce the effective unbalance force, which is the driving the force of contact. The TDB motion control is achieved by using piezoelectric actuation; the demand is the position of the end of the TDB piston.

The effectiveness of the AMB and TDB control is assessed in the steps:

1. The contact-free rotor orbit was established with an unbalanced mass of 7.5 g mounted 35 mm from the center of all three disks. The maximum rotor orbit radius was 0.195 mm, which is within the radial clearance of 0.4 mm.
2. A disturbance force of 600 N was applied to Disk 2 after 1.2 s, lasting for 0.1 s, which was at a sufficient level of impulse to induce rotor/TDB contact.
3. Motion controls on the TDBs to try to recover the rotor to a contact-free levitation by setting them to move in the direction as the rotor at all times under the constraint of TDB radial displacement being limited to 0.1 mm. Control of TDB motion could be initiated at any time.

First, the TDB control was applied to both TDBs, simultaneously at 1.7 s. Figure 4(a) shows the disturbance force, while Figure 4(b) shows the rotor and TDB radial displacements. The rotor dynamics are the same at both TDB locations, which is due to the unbalance distribution symmetry. The rotor radial displacement moves from 0.145 mm (no contact) to full rub at 0.43 mm. The TDB radial displacement moves from no motion to 0.03 mm radial displacement under passive contact forces. Figure 4(c)) shows that the contact force includes significant overshoot to 4,000 N before settling at around 1,600 N on both TDBs. When the active TDB motion is applied to both bearings at the same time, the rotor radial displacement moves to 0.53 mm and the TDB displacement move to 1.3 mm though a transient phase. Figure 4(c) shows the contact force increases to 1,800 N from 1,500 N. The rotor is still in full rub contact with both TDBs. This motion control of the TDBs has increased the rotor and TDB contact displacement together with the contact forces.

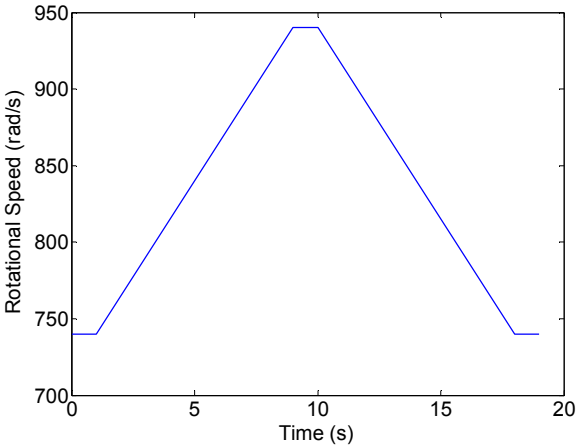

(a) Rotor Operating Speed

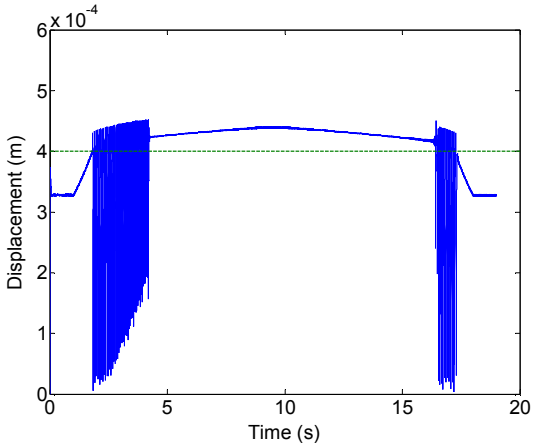

(b) Radial Displacement at TDB-A

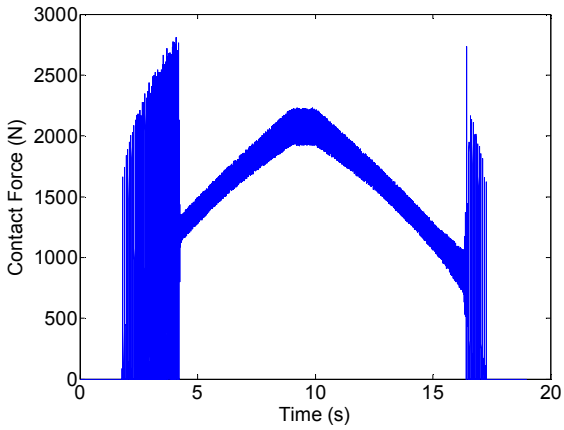

(c) Contact Force at TDB-A

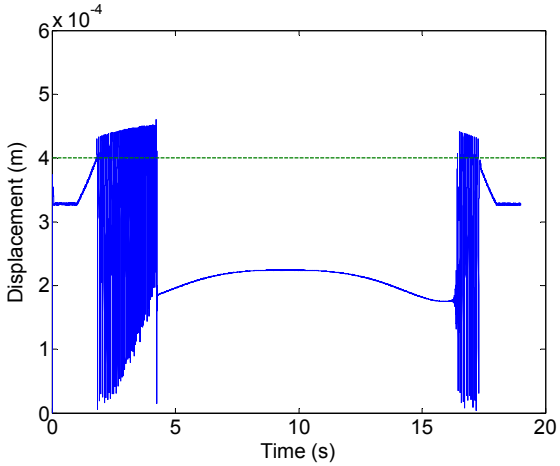

(d) Radial Displacement at TDB-B

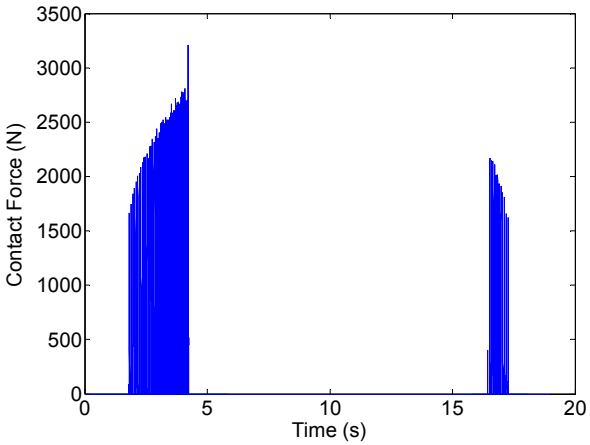

(e) Contact Force at TDB-B

Figure 3: Rotor Time Response Allowing for Rotor and TDB Contact with m_u = 13.5 g

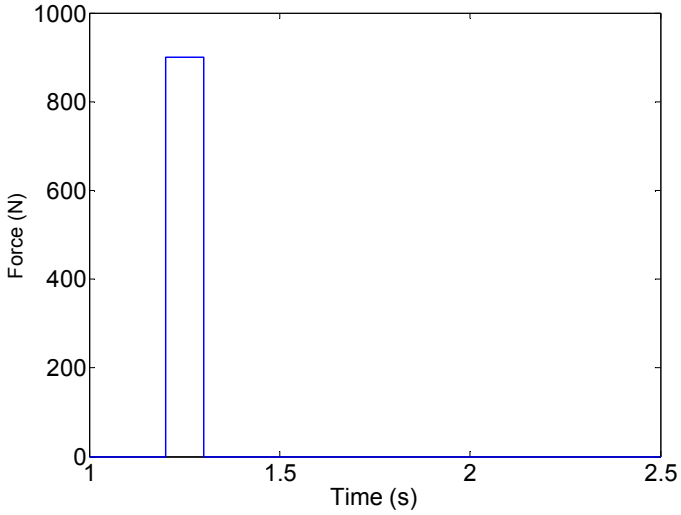

(a) Disturbance Force

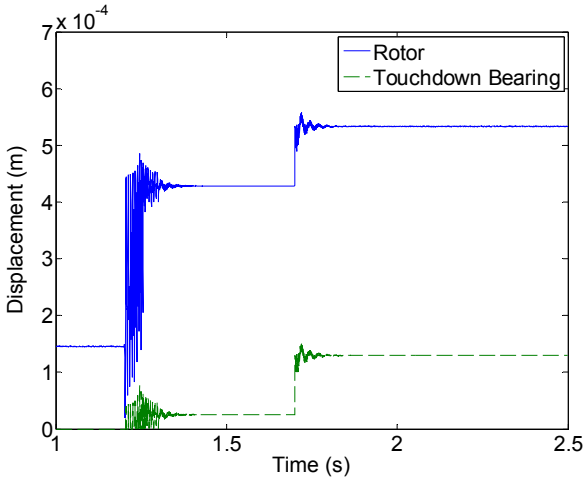

(b) Rotor and TDB Radial Displacement

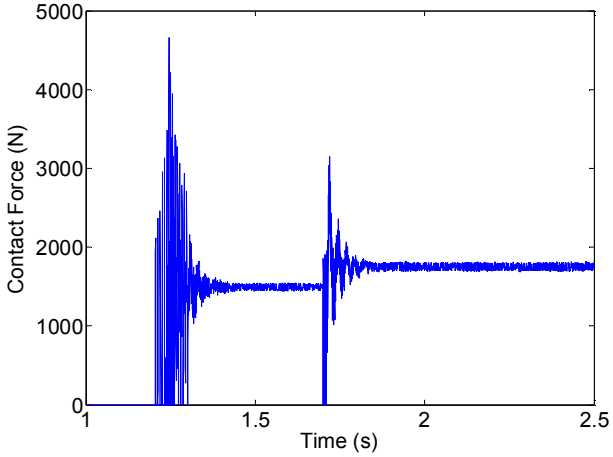

(c) Contact Force

Figure 4: Using Two Active TDBs at the Same Time to Free the Entrapped Rotor with m_u = 7.5 g

Secondly, motion control of TDBs A and B was applied at 1.7 s and 2 s, respectively. Figures 5(a) and 5(c) show the response of rotor and TDB radial displacement at TDBs A and B, respectively. Figures 5(b) and 5(d) show the contact forces at TDBs A and B, respectively. When the control motion is applied to touchdown bearing A at 1.7 s, the contact force reduces to zero in a relatively short time, and rotor contact is lost with TDB-A. However, the contact force between the rotor and TDB-B increases from 1,500 N to 1,600 N, implying heavier contact on TDB-B. At 2 s, the same control motion is applied to TDB-B, the contact force then decreases to zero; hence rotor contact ceases. Applying control on two TDBs at different times appears to be more effective in recovering the rotor to contact-free levitation, when moderate levels of unbalance force exists on the rotor.

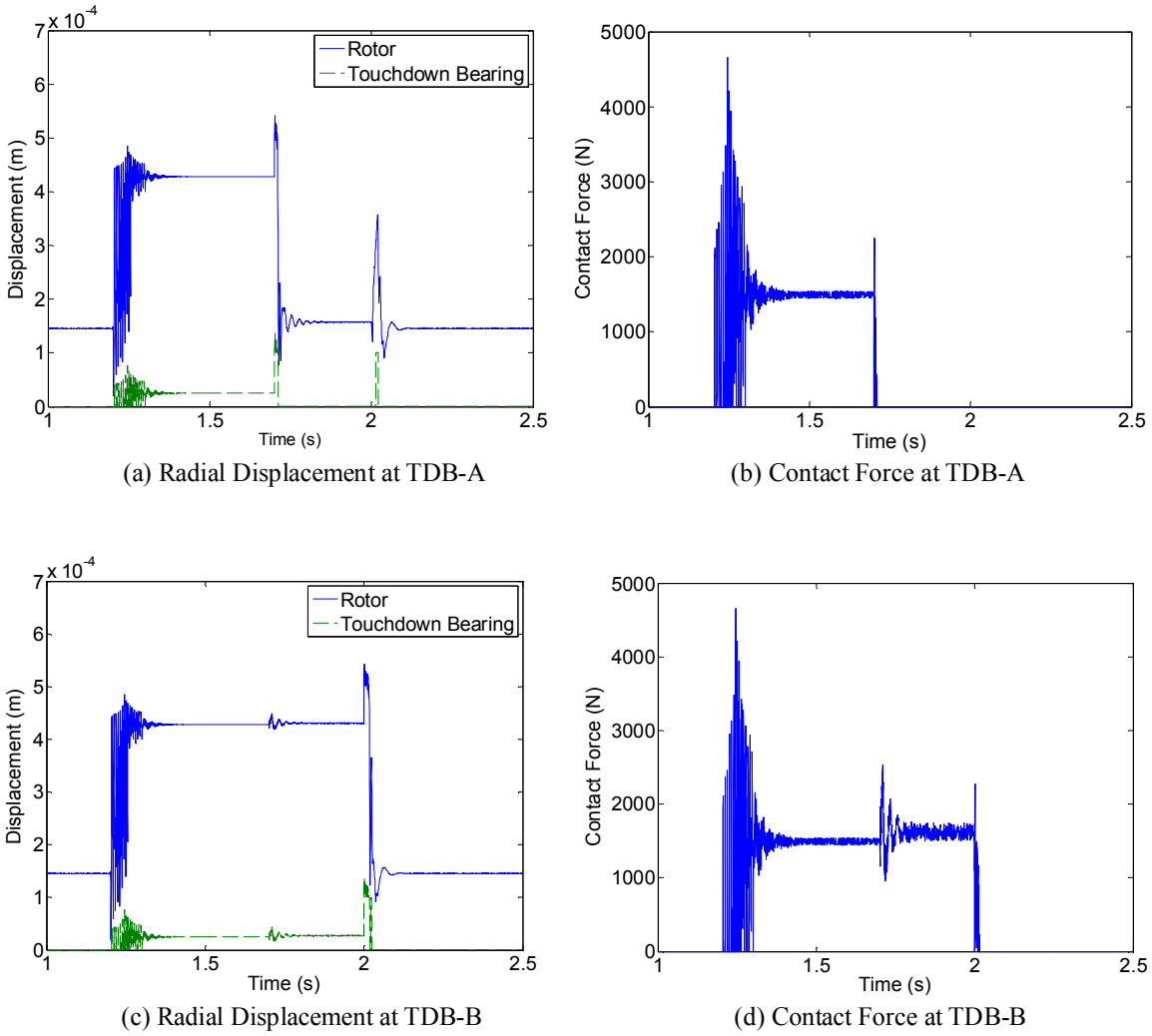

(a) Radial Displacement at TDB-A (b) Contact Force at TDB-A

(c) Radial Displacement at TDB-B (d) Contact Force at TDB-B

Figure 5: Using Two Active Touchdown Bearings Motion at Different Times to Free the Entrapped Rotor with m_u = 7.5 g

The TDB control method was reassessed with higher unbalance masses. The unbalance mass was increased to 10 g on all three disks, then the active motion control was applied to TDB-A at 1.7 s, the results as shown in Figure 6. The contact force decreases over a relatively short time to zero, implying loss of contact on TDB-A. However, the contact force on TDB-B increases to 1,800 N, and full rub contact continues on TDB-B. Afterwards, the same control motion applied to TDB-B results in a higher contact force of 2,100 N. The rotor radial displacement at TDB-B increases to 0.54 mm from 0.43 mm. With the increase in TDB-B motion, it is not possible to bring the rotor to a contact-free condition by using TDB motion control alone.

In order to free the rotor from contact at TDB-B, it is proposed to use AMB force to reduce the effect of unbalance force from Disks 2 and 3. The unbalance force on Disk 1 is not considered; hence the synchronous magnetic bearing force may increase the displacement of the rotor at TDB-A. To assess the control method, two more steps are added to the previous simulation steps:

4. Synchronous AMB forces are applied at 1.8 s to reduce the unbalance force influence from Disks 2 and 3.
5. Synchronous AMB forces are then removed after 2.2 s.

The same steps as the previous simulation are followed; the entrapped rotor at TDB-A is released by applying control motion onto the TDB-A at 1.7 s. When the synchronous forces from the AMBs are applied, Figure 7(d)

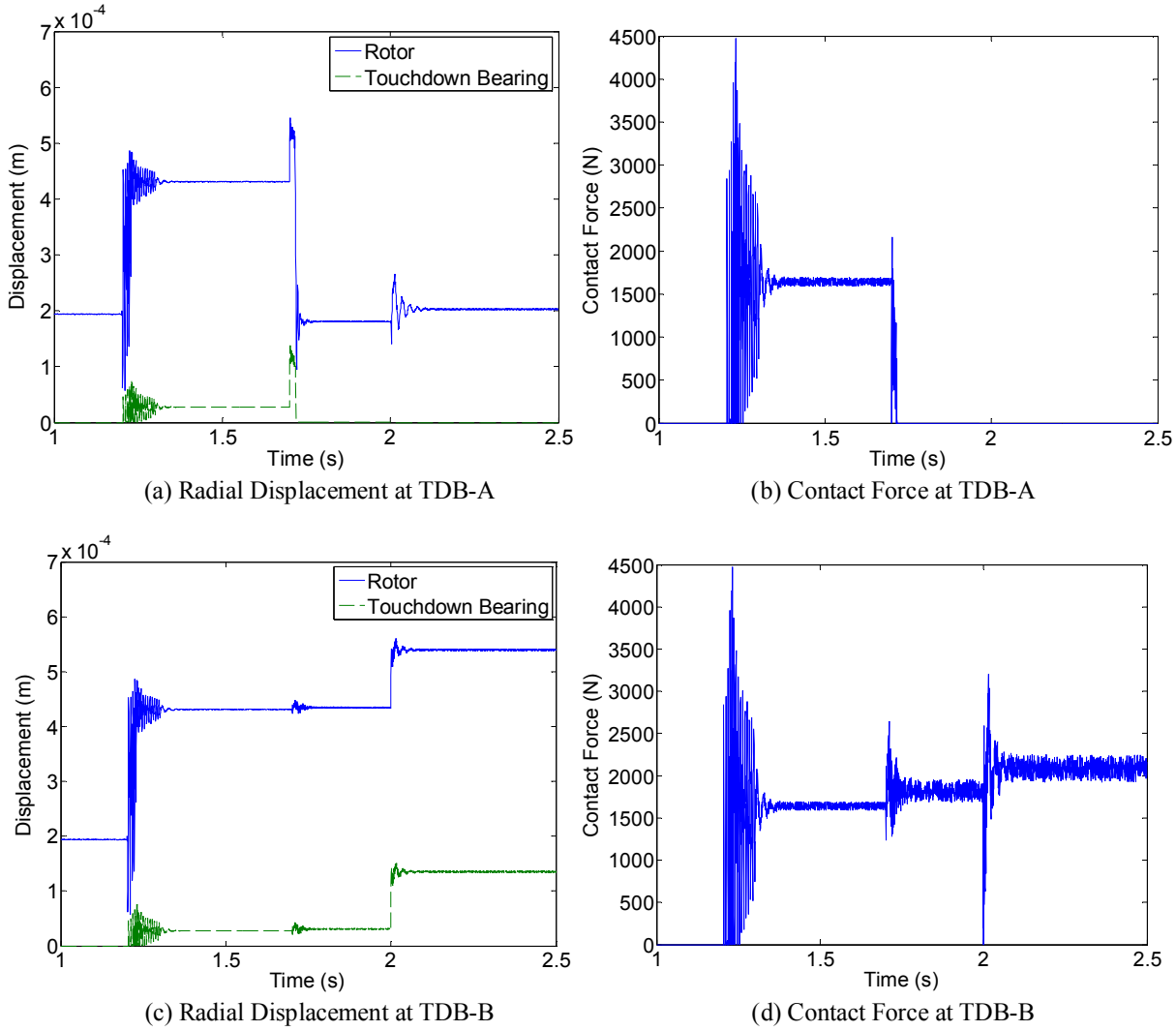

(a) Radial Displacement at TDB-A (b) Contact Force at TDB-A

(c) Radial Displacement at TDB-B (d) Contact Force at TDB-B

Figure 6: Using Two Active TDB Motions at Different Times to Free the Entrapped Rotor with Increased Unbalance Masses (m_u = 10 g)

shows the contact forces on TDB-B reduce to 1,500 N from 1,800 N. Figures 7(a) and 7(c) show the rotor displacement at TDB-B also reduces slightly, while the rotor displacement at TDB-A increases to 0.295 mm. When the control motion of TDB-B is applied at 2 s, Figure 7(d) shows the contact forces to decrease to zero, compared with the increase in contact force in Figure 6(d). Figure 7(c) shows how the synchronous AMB forces and the controlled motion of TDB-B influence the rotor motion. The synchronous AMB force has little impact on the rotor displacement at TDB-B, while the following controlled TDB motion is capable of returning the rotor to contact-free levitation despite the initial increase in displacement. When the synchronous forces from the AMBs are withdrawn, the rotor displacement returns to the level before the initial disturbance force was applied.

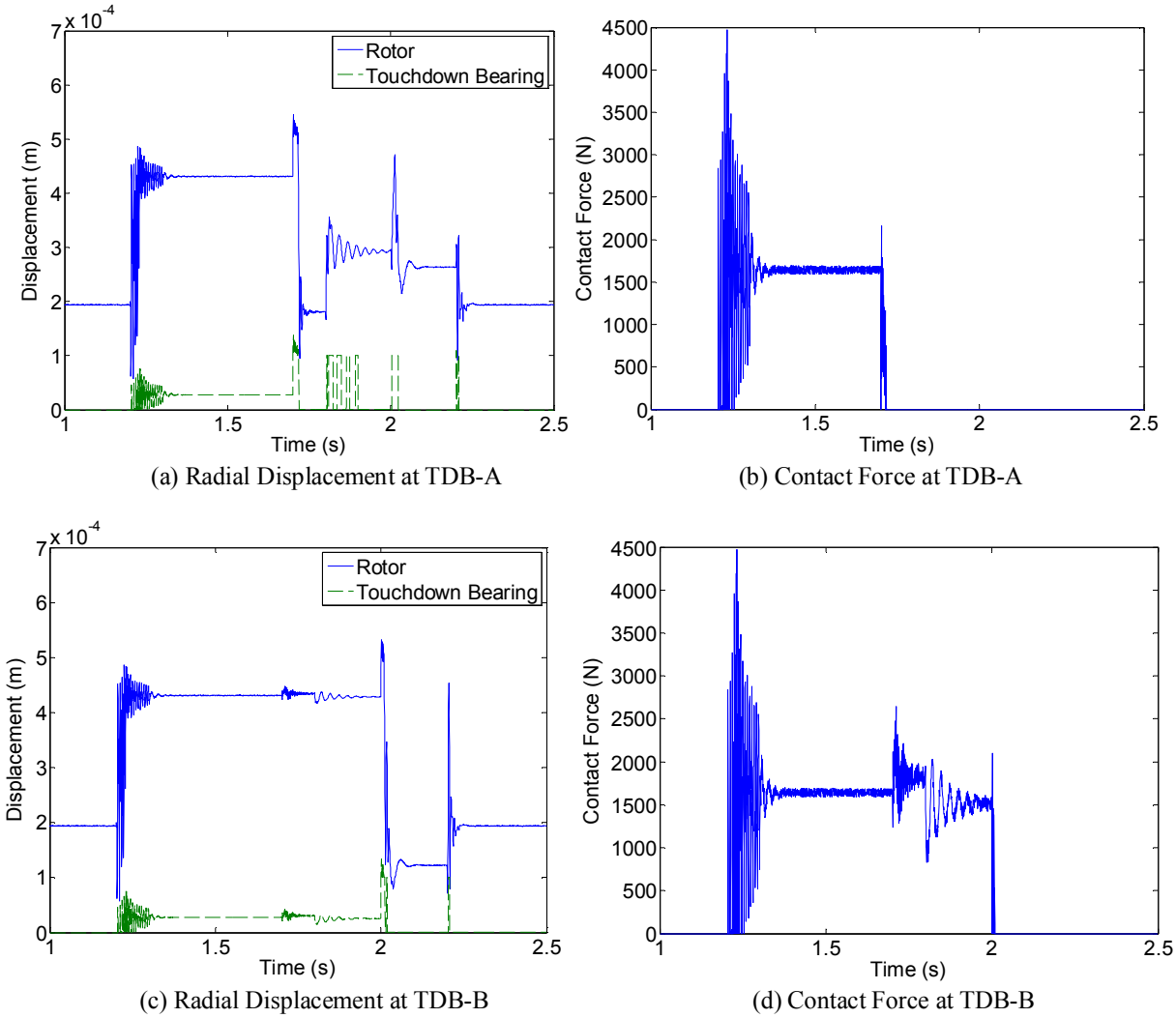

(a) Radial Displacement at TDB-A (b) Contact Force at TDB-A

(c) Radial Displacement at TDB-B (d) Contact Force at TDB-B

Figure 7: Using AMB Control and Two Active TDB Motions at Different Time to Free the Entrapped Rotor with Increased Unbalance Masses ($m_u = 10$ g)

6 Conclusions

This paper has considered the issues associated with an AMB supported flexible unbalanced rotor making contact with TDBs. It has been demonstrated that, for certain levels of unbalance and running speeds, the rotor may co-exist in either a normal contact-free orbit within the clearance circle, or in a persistent condition involving rub or bounce-like contact with one or more TDB. The rotor may undergo the transition from the contact-free orbit to the contact condition if a transient external disturbance is applied to the system. In principle, the reverse transition is possible under another disturbance.

The manner in which a disturbance could be applied to the rotor to encourage it back to the contact-free orbit was then investigated. This is possible using the available control forces from the AMBs and/or by using any active features incorporated into the TDBs. In this paper, a TDB system under piezoelectric actuation was considered. The rotor dynamics under TDB contact are complex and non-linear, which makes definitive control strategies difficult to specify. For certain unbalance distributions, active TDB motion alone may be sufficient. However, at the same running speed, a higher level of unbalance may require active TDB control in tandem with active AMB synchronous control. It may also be beneficial to sequence the control of the active TDBs with appropriate time delays to move to a contact-free orbit.

REFERENCES

[1] Keogh, P.S., Contact Dynamic Phenomena in Rotating Machines: Active/Passive Considerations, Mechanical Systems and Signal Processing 2012.

[2] Johnson, D.C., Synchronous Whirl of a Vertical Shaft Having Clearance in One Bearing, J. Mech. Eng. Sci., Vol.**4**(1), 1962, 85-93.

[3] Ehrich, F.F., Bistable Vibrations of Rotors in a Bearing Clearance. ASME Paper 65-WA/MD-1, 1965.

[4] Black, H.F., Interaction of a Whirling Rotor with a Vibrating Stator Across a Clearance Annulus. J. Mech. Eng. Sci., Vol.**10**(1),1968, 1-12.

[5] Childs, D.W., Rub Induced Parametric Excitation in Rotors. ASME J. Mechanical Design, Vol.**10** (1979), 640-644.

[6] Muszynska, A., Partial Lateral Rotor to Stator Rubs. Paper C281/84, Proc. 3rd Int. Conf. Vibrations in Rotating Machinery, York, UK, Sept. 1984, 327-335.

[7] Choy, F.K., Padovan, J., and Yu, J.C., Full Rubs, Bouncing and Quasi Chaotic Orbits in Rotating Equipment, Journal of the Franklin Institute, Vol.**327** (1990), 25-47.

[8] Lawen, J.L., and Flowers, G.T., Synchronous Dynamics of a Coupled Shaft/Bearing/Housing System with Auxiliary Support from a Clearance Bearing, ASME J. Engineering for Gas Turbines and Power, Vol.**119** (1997), 430-435.

[9] Popprath, S., and Ecker, H., Nonlinear Dynamics of a Rotor Contacting an Elastically Suspended Stator, Journal of Sound and Vibration, Vol.**308** (2007), 767-784.

[10] Schmied, J., and Pradetto, J.C., Behavior of a One Ton Rotor Being Dropped into Auxiliary Bearings, Proc. 3rd Int. Symp. Magnetic Bearings, Alexandria, VA, July 1992, 145-156.

[11] Kirk, R.G., Swanson, E.E., Kavarana, E.H., and Wang, X., Rotor Drop Test Stand for AMB Rotating Machinery, Part 1: Description of Test Stand and Initial Results, Proc. 4th Int. Symp. Magnetic Bearings, ETH Zurich, Aug. 1994, 207-212.

[12] Zeng, S., Modelling and Experimental Study of the Transient Response of an Active Magnetic Bearing Rotor During Rotor Drop on Back-Up Bearings, Part I: Journal of Systems and Control Engineering, Vol.**217**, 2003, 505-517.

[13] Zhu, C., Nonlinear Dynamics of Rotor on Rolling Element Backup Bearings after Active Magnetic Bearing Failure, Chinese Journal of Mechanical Engineering, Vol.**42**, 2006, 196-202.

[14] Hawkins, L. Filatov, A., Imani, S., and Prosser, D., Test Results and Analytical Predictions for Rotor Drop Testing of an Active Magnetic Bearing Expander/Generator, ASME J. Engineering for Gas Turbines and Power, Vol.**129**, 2007, 522-529.

[15] Sun, G., Rotor Drop and Following Thermal Growth Simulations using Detailed Auxiliary Bearing and Damper Models, Journal of Sound and Vibration, Vol.**289**, 2006, 334-359.

[16] Fumagalli, M., Varadi, P., and Schweitzer, G., Impact Dynamics of High Speed Rotors in Retainer Bearings and Measurement Concepts, Proc. 4th Int. Symp. Magnetic Bearings, ETH Zurich, Aug. 1994, 239-244.

[17] Bartha, A.R., Dry Friction Induced Backward Whirl: Theory and Experiment, Proc. 5th IFToMM Conf. Rotor Dynamics, Darmstadt, Sept. 1998, 756-767.

[18] Cuesta, E.N., Rastelli, V.R., Medina, L.U., Montbrun, N.I., and Diaz, S.E., Non-Linear Behaviors in the Motion of a Magnetically Supported Rotor on the Catcher Bearing During Levitation Loss, an Experimental Description, Paper GT-2002-30293, ASME Turbo Expo, Amsterdam, June 2002.

[19] Markert, R., and Wegener, G., Transient Vibration of Elastic Rotors in Retainer Bearings, Proc. ISROMAC-7, Hawaii, Feb. 1998, 764-774.

[20] Kirk, R.G., Gunter, E.J., and Chen, W.J., Rotor Drop Transient Analysis of AMB Machinery, Proc. ASME Int. DETC , Vol.**1B**, 2005, 1003-1012.

[21] Ishii, T., and Kirk, R.G., Transient Response Technique Applied to Active Magnetic Bearing Machinery During Rotor Drop, Journal of Vibration and Acoustics, Vol.**118**, 1996, 154-163.

[22] Keogh, P.S., and Cole, M.O.T., Rotor Vibration with Auxiliary Bearing Contact in Magnetic Bearing Systems, Part 1: Synchronous Dynamics, Proc. Instn Mech. Engrs, Part C, Vol.**217** (2003), 377-392.

[23] Cole, M.O.T., and Keogh, P.S., Rotor Vibration with Auxiliary Bearing Contact in Magnetic Bearing Systems, Part 2: Robust Synchronous Control for Rotor Position Recovery, Proc. Instn Mech. Engrs, Part C, Vol.**217**, 2003, 393-409.

[24] Ulbrich, H., Chavez, A., and Dhima, R., Minimization of Contact Forces in Case of Rotor Rubbing Using an Actively Controlled Auxiliary Bearing, Proc. 10th Int. Symp. Transport Phenomena and Dynamics of Rotating Machinery, Honolulu, Hawaii, March 2004, 1-10.

[25] Ulbrich, H., and Ginzinger, L., Stabilization of a Rubbing Rotor Using a Robust Feedback Control, Paper-ID: 306, Proc. 7th IFToMM Conf. Rotor Dynamics, Vienna, Austria, 2006.
[26] Cade, I.S., Sahinkaya, M.N., Burrows, C.R., and Keogh, P.S., On the Design of an Active Auxiliary Bearing for Rotor/Magnetic Bearing Bystems, Proc. 11th Int. Symp. Magnetic Bearings, Nara, Japan, Sept. 2008.
[27] Keogh, P.S., Sahinkaya, M.N., Burrows, C.R., and Cade, I.S., Rotor/Auxiliary Bearing Dynamic Contact Modes in Magnetic Bearing Systems, Proc. 11th Int. Symp. Magnetic Bearings, Nara, Japan, Sept. 2008.
[28] Nelson, H.D., and McVaugh, J.M., Dynamics of Rotor-Bearing Systems Using Finite-Elements, J. Engineering for Industry-Transaction of the ASME, Vol.**98**(2), 1976, 593-600.
[29] Burrows, C.R., and Sahinkaya, M.N., Vibration Control of Multi-Mode Rotor-Bearing Systems, Proceedings. Royal Society of London, Series A, Mathematical and Physical Science, Vol. **386**, 1983, 77-94.
[30] Burrows C.R., Sahinkaya M.N., and Clements S., Active Vibration Control of Flexible Rotors: An Experimental and Theoretical Study, Proc. Royal Society, London, **A422**, 1989, 123-146.